Journal of Molecular Catalysis A: Chemical 314 (2009) 35–41

Contents lists available at ScienceDirect

Journal of Molecular Catalysis A: Chemical

journal homepage: www.elsevier.com/locate/molcata

Preparation, characterization and visible-light activity of carbon modified TiO_2 with two kinds of carbonaceous species

Chao Chen [a], Mingce Long [b,*], Hui Zeng [b], Weimin Cai [a,b,**], Baoxue Zhou [a,b], Jingyi Zhang [b], Yahui Wu [a], Dawei Ding [b], Deyong Wu [b]

[a] Department of Environmental Science and Engineering, School of Municipal and Environmental Engineering, Harbin Institute of Technology, Harbin 150090, People's Republic of China
[b] School of Environmental Science and Engineering, Shanghai Jiao Tong University, Dong Chuan Road 800, Shanghai 200240, People's Republic of China

ARTICLE INFO

Article history:
Received 23 April 2009
Received in revised form 23 July 2009
Accepted 14 August 2009
Available online 22 August 2009

Keywords:
Photocatalysis
Titanium dioxide
Visible light
Carbon modified

ABSTRACT

Visible-light responsive carbon modified TiO_2 was synthesized through simple precipitation of tetrabutyl titanate in proper amount of water. The as-synthesized catalyst was characterized by elemental analysis, N_2 adsorption–desorption analysis, X-ray powder diffraction (XRD), Raman spectroscopy, transmission electron microscopy (TEM), X-ray photoelectron spectroscopy (XPS), UV–vis diffuse reflectance spectra (DRS) and nuclear magnetic resonance (NMR). The results indicate that carbon modifies TiO_2 in two ways: doping as interstitial carbon in the crystal lattice and coating as graphite-like carbon on the surface. It is found that the interstitial carbon could narrow the band gap, and the graphite-like carbon could serve as sensitizer. The sensitization effect of graphite-like carbon is found to contribute greatly to the excellent photocatalytic performance of carbon modified TiO_2. It has been found that 95.6% of MO was decolorized within 120 min and 92.7% of Cr(VI) was reduced within 90 min in the presence of phenol. The formation mechanism of the carbon modified TiO_2 has been discussed.

1. Introduction

Semiconductor photocatalysis is one of the most promising technologies in providing clean hydrogen energy and removing recalcitrant organic pollutant [1–3]. Although hundreds of new compounds with diverse photocatalytic performance have been developed [4], titanium dioxide is still the most popular one due to its effectiveness, cheapness and chemical stability [5–7]. Thereby TiO_2 is especially suitable for the application in environmental remediation [1]. However, the main bottle neck for TiO_2 widespread adoption is that TiO_2 can only be activated by UV light (about 3–5% of solar light) because of its wide band gap. In order to conquer this problem, some strategies have been explored to extend the optical response into the visible region, e.g. metal doping [8], nonmetal doping [9–11], transition metal compound or dye sensitizing [12–15]. Since Asahi reported the visible-light photocatalytic activity of nitrogen-doped TiO_2 [9], doping TiO_2 with N, C, S, I and other nonmetal elements has become more and more attractive. However, there also remains disputation on the chemical states of the doping species [16] and the origin of the visible-light driven photoactivity [17–19].

Carbon modified TiO_2 has always attracted much attention for its outstanding photocatalytic activity [20–34]. In fact there are three kinds of carbon modified TiO_2. The first kind is carbon-doped TiO_2, in which the carbon substitutes oxygen or titanium or presents as interstitial species in the lattice. A large number of approaches have been developed to obtain the carbon-doped TiO_2: flame pyrolysis of Ti metal sheet [20], oxidative annealing of TiC powder [21] or oxidization of TiC at low temperature with nitric acid [22], hydrothermal treatment of amorphous TiO_2 with glucose [23], direct solution-phase carbonization using $TiCl_4$ and diethanolamine as precursors [24], nonhydrolytic sol–gel method followed by annealing [25], sol–gel auto-combustion method [26] and hydrolysis of $TiCl_4$ with tetrabutylammonium hydroxide followed by prolonged heating [27]. The second kind of carbon modified TiO_2 is carbon coated TiO_2. Toyoda et al. reported a carbon-coated Ti_nO_{2n-1} by heat treatment of TiO_2 and poly(vinyl alcohol) in inert atmosphere [30]; Lettmann et al. reported a coke containing titanium dioxide via acid-catalyzed sol–gel process [31]; and Zhang et al. reported the surface hybridization of TiO_2 with graphite-like carbon layer through hydrothermal treatment of P25 TiO_2 with glucose followed by graphitization of the carbonaceous species [32]. The third kind of carbon modified TiO_2 is the TiO_2

* Corresponding author. Tel.: +86 21 54747354; fax: +86 21 54740825.
** Corresponding author. Tel.: +86 21 54748019; fax: +86 21 54748019.
E-mail addresses: long_mc@sjtu.edu.cn (M. Long), wmcai@sjtu.edu.cn (W. Cai).

1381-1169/$ – see front matter © 2009 Elsevier B.V. All rights reserved.
doi:10.1016/j.molcata.2009.08.014

loaded activated carbon. Enhanced photocatalytic performance is observed for the TiO_2 loaded activated carbon due to the improved adsorption [33,34]. However, this type of carbon modified TiO_2 cannot response to visible light.

Carbon elements in carbon-doped TiO_2 and carbon coated TiO_2 play different roles on the optical response properties. According to the density functional theory (DFT) calculation, substitutional (to O) or interstitial carbon of carbon-doped rutile or anatase TiO_2 introduces a series of localized occupied states in the band gap, contributing to the observed red shift of absorption edge [29]. However, the carbonaceous species on the surface of TiO_2 could act as photosensitizer [31] or promote the photogenerated charge separation by means of electron coupling of π states of graphite-like carbon and the conduction band states of TiO_2 [32].

Carbon modified TiO_2 possesses a wide optical absorption, covering a large part of solar spectrum; therefore it is promising in the solar energy utilization. Much effort should be exerted to develop facile approaches to synthesize efficient carbon modified TiO_2. Herein we propose a new and simple method which is composed of hydrolysis and precipitation of tetrabutyl titanate in proper amount of water and subsequent calcination in presence of deficient oxygen. The carbon was found to exist both in the crystal lattice and on the surface, and the formation mechanism was also tentatively discussed.

2. Experimental

2.1. Sample preparation

Carbon modified TiO_2 samples were synthesized by a facile hydrolysis–precipitation–calcination approach. In a typical procedure, tetrabutyl titanate ($Ti(OBu)_4$) (Shanghai Reagent Corporation) was dropwise added into deionized water under modest stir, and the molecular ratio of Ti to H_2O is 1:20. Subsequently, the suspension solution was stirred for another 10 min to continue hydrolysis and polycondensation. A xerogel was obtained by drying the mixture under air at 80 °C. The grounded powder was put into a homemade apparatus and calcined in a muffle furnace. The homemade apparatus was composed of a 50 ml round bottom flask and a modified schlenk tube without a sidearm but a 2 mm hole. They were connected via ground glass joint, and during calcination samples were put in the bottom round flask. The temperature was raised up to 350 °C with a heating rate of 5 K/min and kept for one hour. A cleaning process involving four cycles of centrifugation/washing/re-dispersion in water was applied to the resulted powder. Finally the fine catalyst powder was achieved after dried and crushed. The sample prepared without calcination was named S0 and other catalysts were named in the form of S-t (*t* represents the calcination temperature). Degussa P25 has been tested as a comparison.

2.2. Characterization

X-ray diffraction analysis was carried out using a Rigaku D/Max-2200/PC X-ray diffractometer with Cu Kα radiation at 40 kV and 20 mA, and the diffraction angle 2θ was scanned in 5–80° with step of 0.02°. The micrograph of the particles was observed by a high resolution-transmission electron microscopy (HRTEM, JEM100-CX JEOL). X-ray photoelectron spectroscopy measurements were performed on a RBD upgraded PHI-5000C ESCA system (Perkin Elmer), and Ar^+ ion beam with an accelerating voltage of 3 kV, a beam current of 10 mA and an etching time of 15 min was used to etch the sample. UV–vis diffuse reflectance spectra were recorded on a TU-1901 UV/vis spectrophotometer (Beijing purkinje general instrument Co., Ltd., China) and converted from reflection to absorption by the Kubelka-Munk method. The specific surface area and pore size distribution were measured employing a Nova 100 (Quantachrome Instruments) with nitrogen as the adsorption gas. Fourier transform infrared spectroscopy (FTIR) was performed on an IR Prestige-21 system (Shimadzu Corporation, Japan). Raman spectra were measured with a LabRam-1B Raman microspectrometer at 632.8 nm (Horiba Jobin Yvon, France). The carbon element content was studied by a Dekai HCS-040G Carbon-Sulfur Analyzer (Dekai Instruments, China). ^{14}C MAS NMR spectra were acquired in a wide-bore Brucker Avance III 400 spectrometer at 9.4 T with a CP/MAS solid broadband probe head.

2.3. Photocatalytic activity

The optical system for the photocatalytic reaction consists a 1000 W xenon lamp and a cutoff filter ($\lambda > 400$ nm or $\lambda > 510$ nm). If there is no special illustration, most reactions were conducted under irradiation above 400 nm. The photocatalytic activity of the samples was evaluated by the degradation of methyl orange (MO) and the reduction of chromium(VI). In a typical test for MO degradation, 0.05 g catalyst was added into 50 ml MO solution (12 mg/l) to get a suspension, then the suspension was treated with ultrasonic for 5 min and stirred in dark for 15 min to reach a balance of adsorption and desorption. Then the light was switched on, and samples were taken, separated and analyzed at regular time intervals. The effect of adsorption over S350 was also studied under the same experiment condition but without irradiation. The concentration of MO was monitored with a UNICO UV-2102 spectrometer at 464 nm. The test for chromium(VI) reduction was carried out by mixing 0.025 g carbon modified TiO_2 with 50 ml aqueous solution containing 56.6 mg/l $K_2Cr_2O_7$ and 37.6 mg/l phenol. The initial pH of the suspension was adjusted by sulfuric acid to around 2.0. Then the suspension was treated and sampled following the same procedures as that of MO degradation. The concentration of Cr(VI) and phenol were analyzed by the spectrophotometric method of the diphenylcarbazide at 540 nm and 4-Aminoantipyrine at 510 nm, respectively. Stability tests for MO degradation have been carried out. The method was that 100 ml solution was used for test, and after every two hours reaction, the catalyst was transferred out from solution, dried in oven at 80 °C and then grounded for next cycle. In every cycle, the concentrations of catalyst and methyl orange were kept constant.

3. Results and discussion

3.1. Catalyst characterization

Fig. 1 shows the XRD patterns of the samples calcined at different temperatures. The presence of exclusive anatase phase of titanium dioxide can be observed (JCPDS, No. 21-1272) in all of these calcined samples. It should be underlined that anatase phase appears at as low temperature as 250 °C in our study, which is quite different from that of the previous report [35]. Normally anatase phase appears when the pure amorphous TiO_2 calcined at temperature higher than 350 °C, and often be accompanied by brookite. According to the result of elemental analysis, the carbon content in the S0 is about 5.00 wt.%. To determine the source of carbon in the sample, the ^{13}C NMR spectrum was measured (Fig. 2). The spectrum shows the signals of four carbons from 1-butanol (the hydrolysis product), which are at 62.9, 34.5, 18.7 and 12.9 ppm [36]. And the signals from 76.7 to 79.6 ppm come from the first carbon connecting with oxygen in the -Ti-(O-C_4H_9) group, which is 74.8 ppm for that of tetrabutyl titanate [36]. It suggests that in the amorphous xerogel there are considerable amount of adsorbed 1-butanol and tetrabutyl groups at the terminal of the titania network. Therefore

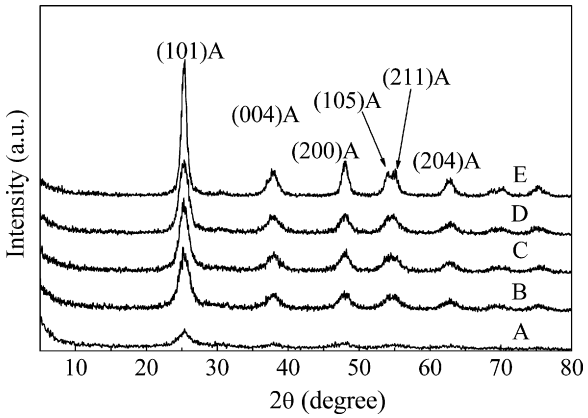

Fig. 1. XRD patterns of the carbon modified TiO_2 (a) S0, (b) S250, (c) S300, (d) S350 and (e) S450.

the presence of carbon species inhibits the formation of brookite [23].

The peak intensity increases and the width of the (1 0 1) plane diffraction peak becomes narrower as the calcination temperature increases. It suggests that the crystallinity is improved. The average particle sizes are calculated from the full widths at half-maximum of the (1 0 1) peak by applying the Scherrer equation (grain size, $d = 0.9\lambda/(\beta \cos\theta)$, where λ is the characteristic X-ray wavelength applied (0.1545 nm), β is the half width of the peak at the 2θ value and 0.9 is the apparatus constant). The average particle sizes of 5.4, 7.7, 9.7 and 16.9 nm are obtained for S250, S300, S350 and S450, respectively. It corresponds to the well-known results that the particle size grows up as calcination temperature increases [37].

The HRTEM image of the sample S350 is displayed in Fig. 3. The nano-crystallines with sizes of 10 nm agglomerate together, holding a microporous structure formed during the disordered accumulation. The size of the nano-crystalline is in consistent with the calculated value obtained from XRD patterns. The small size of TiO_2 nano-crystalline might be attributed to the presence of carbon inhibiting the enlargement of particles. In fact the carbon content in S350 is measured as 2.49 wt.% by the elemental analysis, and the value is even higher than the one estimated from XPS by Khan [20]. Moreover according to the ^{13}C NMR test there is no carbon signal observed in the sample, which excludes the C-H group existence. It can be sure that the soluble matter has been removed by the final washing process. Raman spectrum of S350 was tested to further investigate the carbon species. From Fig. 4, peaks at 144, 397, 518 and 639 cm^{-1} are typical of anatase TiO_2 [38]. Two peaks around 1582 and 1100 cm^{-1} indicate the existence of amorphous carbons with some degrees of graphitic ordering [39]. Therefore the

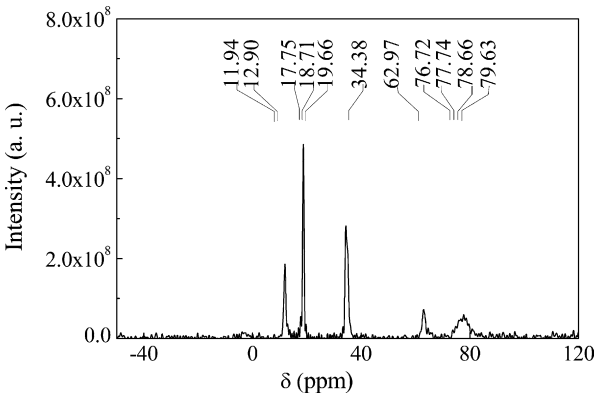

Fig. 2. ^{13}C NMR spectrum of the sample S0.

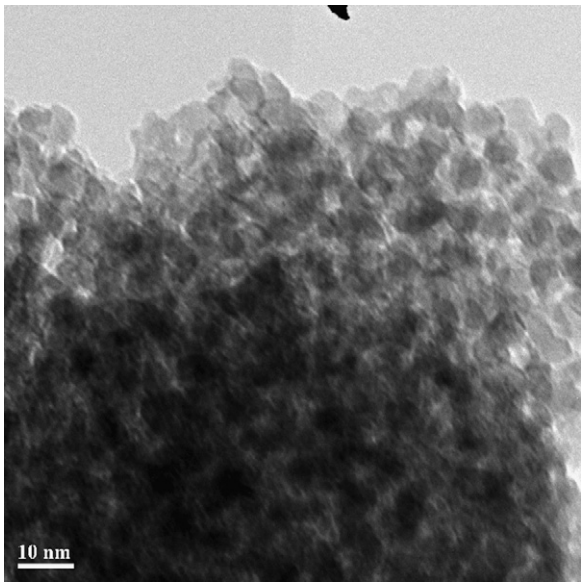

Fig. 3. TEM image of the carbon modified TiO_2 S350.

remained carbon on the surface of the crystalline must be present as a stable graphite-like carbonaceous species.

The XPS measurement was carried out to establish the chemical state of the elements in the sample S350. Ar^+ ion etching ($S350_{Ar}$) was performed to investigate the difference between surface and bulk region. The XPS results are shown in Fig. 5. It displays that S350 only contain Ti, O and C with peaks around 458 eV (Ti *2p*), 531 eV (O *1s*) and 285 eV (C *1s*), respectively. The binding energy of C *1s* at 284.6 eV is used to calibrate all of the obtained data. Fig. 5a shows the high resolution C *1s* core-level XPS spectra of the S350 and $S350_{Ar}$. There are three peaks at 284.6, 285.6 and 288.6 eV in S350 and only two peaks at 284.6 and 286.6 eV in $S350_{Ar}$. The peak at 284.6 eV can be assigned to the adventitious carbon contamination adsorbed from the ambient. The peak around 285.6 eV is ascribed to element carbon [40,41], which possesses the same binding energy as that of graphite intercalation compound. The disappearance of this peak in $S350_{Ar}$ suggests that the element carbon exists on the surface of the sample. Considering Raman results of the existing carbon with some degree of graphitic ordering, the surface element carbon could be attributed to a kind of graphite-like structure carbon. The peak at 288.6 eV can be attributed to carbonate species, the same as many reports of cation C^{4+}-doped TiO_2 [22,26]. Normally there are two different kinds of doped carbons in the reference work. The one is the anion-doped carbon which was regarded as

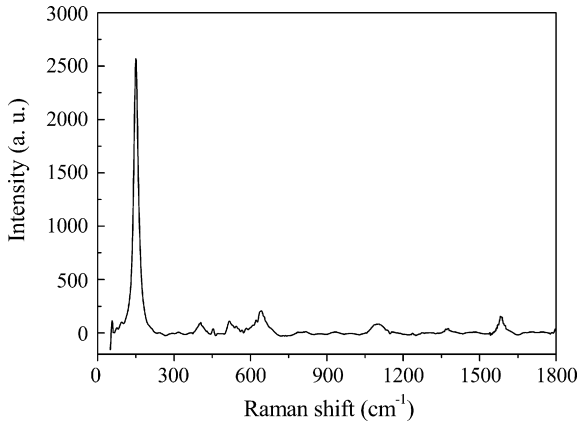

Fig. 4. Raman spectra of carbon modified TiO_2 S350.

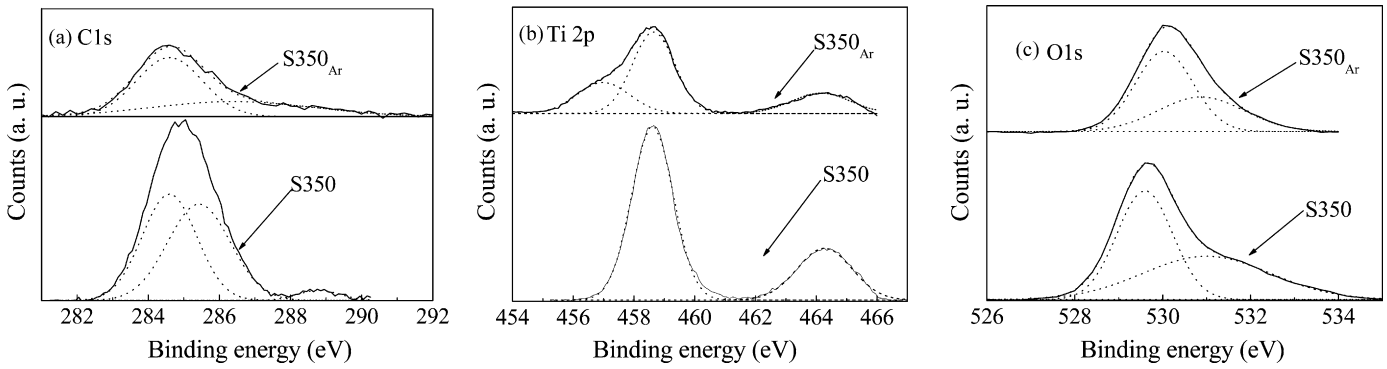

Fig. 5. XPS spectra for carbon modified TiO_2 S350 and $S350_{Ar}$: (a) C *1s*, (b) Ti *2p* and (c) O *2p*.

substitutional carbon for oxygen with the XPS peaks at 281–282 eV. The other one is the cation-doped carbon which was regarded as carbonate matters with the XPS peaks at 288–289 eV. By theoretic calculation, Kamisaka et al. [42] proposed that the carbonate doping matter is formed from the substitute carbon for Ti. Another calculation by Di Valentin [29] confirmed that the substitution for Ti would induce strong distortion. In our opinion, the substitute for Ti is impossible due to the big difference of ionic radius of C^{4+} and Ti^{4+}, 0.16 and 0.68, respectively. In this work the peak at 288.6 eV is completely removed by Ar^+ ion etching, indicating that the carbonate species only exist on the surface. However, a new peak emerging at 286.6 eV in $S350_{Ar}$ suggests the existence of C—O bond [37] in bulk region of S350, which could originate from either substitutional (to Ti) carbon or interstitial carbon. The lower binding energy than that of carbonate species suggests a lower valence of the carbon, which might be surrounded by both oxygen and titanium atoms. Therefore it is more proper to attribute the doped carbon to the interstitial one.

The XPS spectra of Ti *2p* and O *1s* regions are shown in Fig. 5b and c. The peaks around 458.5 and 464.2 eV are ascribed to Ti $2p_{3/2}$ and Ti $2p_{1/2}$ of TiO_2 (Fig. 5b) [43], respectively. The absence of peaks at binding energy lower than 458.1 eV [26] suggests that titanium exists only as Ti^{4+}. However, the additional peak at 457.04 eV of $S350_{Ar}$ shows the existence of Ti^{3+} in the bulk region [44]. In addition, O *1s* peaks corresponding to the lattice oxygen of TiO_2 are located at 529.74 and 530.09 eV for S350 and $S350_{Ar}$, respectively. It shifts positively after Ar^+ ion etching. This can be understood by the fact that sputtering with Ar^+ ion can partially reduce Ti^{4+} to Ti^{3+} and Ti^{2+} and lead to the shift of the O *1s* peak to a higher binding energy [45–47].

FTIR spectra of the samples are shown in Fig. 6. In all of these samples, a broad band between 3000 and 3600 cm^{-1}, centering about 3421 cm^{-1} which is ascribed to the O-H stretching vibrations of surface hydroxyl groups and molecularly adsorbed water can be observed [48]. The band around 1620 cm^{-1} is another support for the H-O-H bending vibrations of the molecularly adsorbed water [49]. The absence of characteristic bands of tetrabutyl titanium below 1126 cm^{-1} indicates the disappearance of such groups as Ti—O—C [50]. However, there are many disordered spikes from 1400 to 1900 cm^{-1}, which always relate to the graphite-like matter in the carbonization process, which has also been proved by XPS and Raman analysis.

The colors of samples S250, S300 and S350 are gray; however, the sample S450 is almost white. Their optical properties were measured by the UV–vis diffuse reflectance spectra, and the results are displayed in Fig. 7. The indirect band-gap energies of the particles are estimated from the intercept of the tangent in the plots of $(\alpha h\nu)^{1/2}$ versus photon energy ($h\nu$). And the resulted band-gap energies are 3.23, 2.60, 2.72, 3.06 and 3.16 eV for S0, S250, S300, S350 and S450, respectively. It can be inferred that the C *2p*

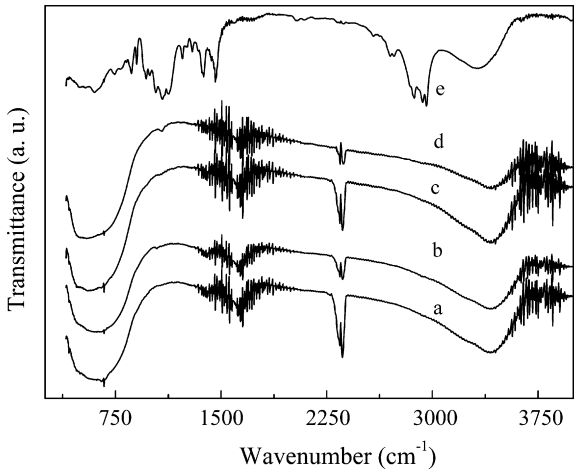

Fig. 6. FTIR spectra for carbon modified TiO_2 (a) S250, (b) S300, (c) S350, (d) S450 and (e) tetrabutyl titanium.

from the interstitial carbon could hybridize with O *2p* to form an upshift valence band and then narrow the band gap [51]. In addition, the long tracks below the band-gap energies of S250, S300 and S350 indicate that the absorbance extends to the wavelength even larger than 600 nm. These track absorptions are caused by the surface graphite-like carbon, but the narrower band-gap energies are attributed to the doped carbon in the lattice. Moreover, with increase of the calcination temperature, the track absorptions decrease and the band-gap energies enlarge. It indicates that at higher temperature surface graphite-like carbon can be oxidized,

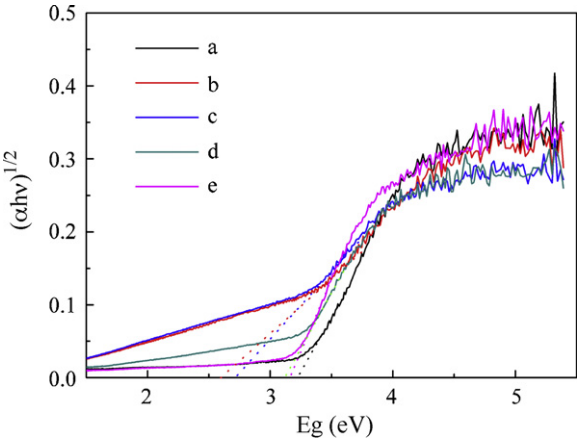

Fig. 7. UV–vis diffuse reflectance spectra for carbon modified TiO_2: (a) S0, (b) S250, (c) S300, (d) S350 and (e) S450.

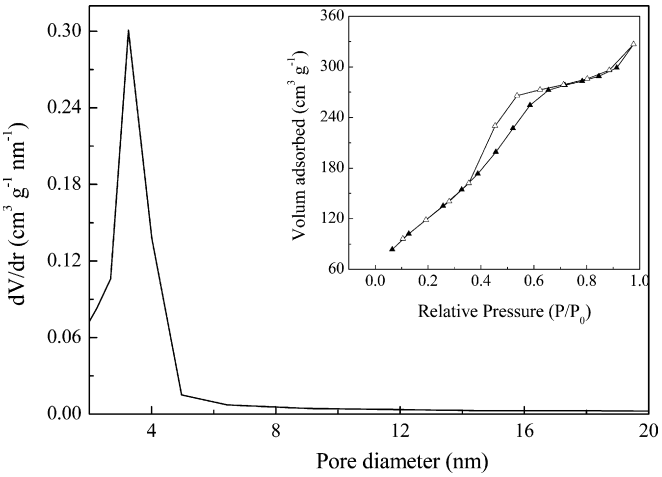

Fig. 8. BJH pore size distribution plots and N_2 adsorption–desorption isotherms (insert) of carbon modified TiO_2 S350.

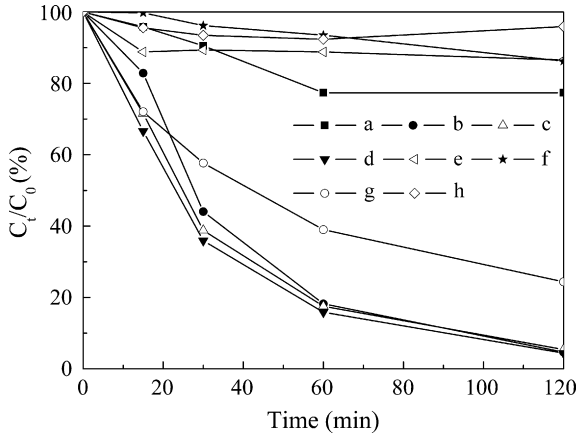

Fig. 9. Degradation of methyl orange with photocatalyst (a) S0, (b) S250, (c) S300, (d) S350, (e) S450 and (f) P25 under irradiation above 400 nm; (g) S350 under irradiation above 510 nm and (h) adsorption of MO by S350 without irradiation (1 g/l of catalyst, 12 mg/l of methyl orange).

and the doped carbon can also be driven out by the presence of oxygen.

Fig. 8 shows the pore size distribution curve of S350 calculated from the desorption branch of the nitrogen isotherm by the Barrett–Joyner–Halenda (BJH) method, and the corresponding nitrogen adsorption–desorption isotherms are shown in the illustration inset. The sample exhibits a Type IV adsorption isotherm with a H_2 hysteresis loop, which demonstrates a diffusion bottleneck, possibly caused by nonuniform pore size. The pore size distribution shows a narrow pore size range of 2.0–6.0 nm and centres around 3.3 nm. The BET specific surface area of S350 was 481 m^2/g. The relatively large surface area is favorable for an excellent photocatalytic performance.

3.2. Formation mechanism of carbon modified TiO_2

The process of hydrolysis and polycondensation of titanate has been discussed extensively [52–54]. The discussion is based on a presumption that the titanium containing precursor is hydrolyzed completely without any carbonaceous species residues in the polycondensed network. However, according to our NMR observation, there are considerable amount of ester bonds connected carbon in the sample S0 and a lot of surface adsorbed 1-butanol. The signals of the first carbon connecting with oxygen in the -Ti-(O-C_4H_9) group show slight shifts (Fig. 2), and it could be inferred that this might be caused by Ti—O—Ti network. The adsorption of 1-butanol performs a strong action similar to that of the surface adsorbed water, and a large amount of hydrogen bonds exist in the structure. Therefore the rapid precipitation process when titanium alkoxides add into water can be described as followed. The titanium alkoxides, $Ti(OR)_4$ (R = alkyl group), hydrolyze with water to form hydroxyl ester and alcohol (Eqs. (1) and (2)). The unstable hydroxyl esters undergo dehydrative or dealcoholic polycondensation to form Ti—O—Ti bond, and develop into three-dimensional network structure following Eq. (3). It should be noted that the hydrolysis and polycondensation are very fast and proceed simultaneously. Finally amorphous TiO_2 precipitation is obtained accompanied with the ending of particle growth. The unit structures with a terminal alkoxyl group and an adsorbed alcohol are depicted in Scheme 1. When the precipitation is calcined under oxygen-poor condition, the carbonaceous species in the network can be easily incorporated into the TiO_2 crystal lattice to form interstitial carbonaceous species, or form graphite-like carbon on surface connecting closely with the TiO_2 lattice via a carbonization process.

$$Ti(OR)_4 + H_2O \rightarrow HO\text{-}Ti(OR)_3 + ROH \quad (1)$$

$$Ti(OR)_4 + nH_2O \rightarrow (HO)_n\text{-}Ti\text{-}(OR)_{4-n} + nROH \quad (n \leq 4) \quad (2)$$

$$(OR)_{4-n}(OH)_{n-1}Ti\text{-}OH + XO\text{-}Ti(OH)_n(OR)_{3-n} \rightarrow (OR)_{4-n}(OH)_{n-1}Ti\text{—}O\text{—}Ti(OR)_{3-n}(OH)_n + XOH \quad (X = H \text{ or } R) \quad (3)$$

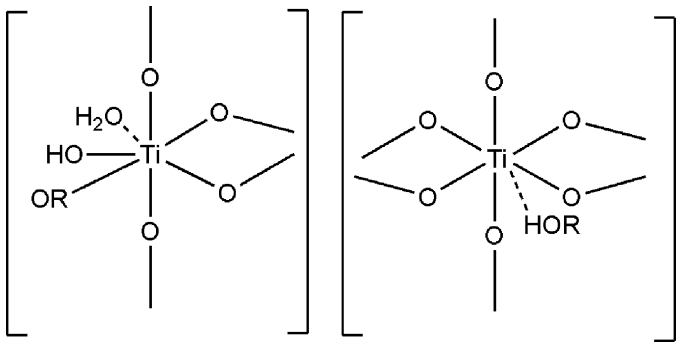

Scheme 1. Unit structure with carbon species in the sample S0.

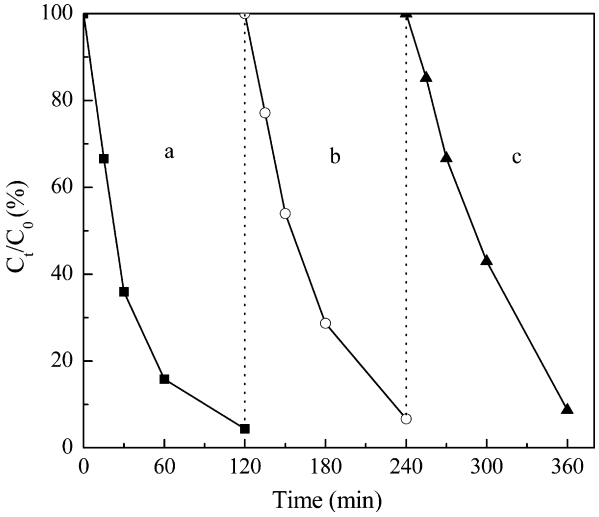

Fig. 10. Photoactivity stability test of S350 in decolorizing methyl orange: (a) first run, (b) second run, (c) third run (irradiation above 400 nm, 1 g/l catalyst, 12 mg/l methyl orange).

Table 1
Results on Cr(VI) reduction[a].

Reaction conditions	Irradiation[b], S350[c], phenol[d]	Irradiation[b], phenol[d]	S350[c], phenol[d]	Irradiation[b], S350[c]
Cr(VI) reduction efficiency after 90 min reaction (%)	92.7	0	0	45.7
k_{obs} (min^{-1})	0.028	0	0	0.009

[a] Cr(VI) concentration = 20 mg/l.
[b] Irradiation with λ > 400 nm.
[c] Catalyst amount = 0.5 g/l.
[d] Phenol concentration = 37.6 mg/l.

3.3. Photocatalytic activity

Fig. 9 shows the photocatalytic activity of the as-synthesized samples in the decolorization of MO. As can be seen from the curve *f*, Degussa P25 exhibits very low photoactivity under visible-light irradiation, which is attributed to the well-known wide band gap of TiO_2. It also confirms that the decolorization of MO by dye sensitization could be negligible under our experimental condition. The MO decreased very little over the amorphous sample S0, because significant recombination of photogenerated electron and hole occurred due to its poor crystallinity. However, in the presence of the sample S250, S300 and S350, more than 90% of MO decreased within 120 min under visible-light irradiation. All these samples hold similar activities, and S350 is slightly better. The surprising high activity could be caused by the sensitization effect of surface graphite-like carbon, the adsorption effect of surface graphite-like carbon and the band gap narrowing effect of the doped carbon. The adsorption effect could be excluded because of the negligible adsorption observed over S350 (curve h). S350 was used to decolorize MO under irradiation above 510 nm, which could only excite the semiconductor with band gap narrower than 2.43 eV. However, about 75.6% of MO has been degraded, which suggests that sensitization effect of surface graphite-like carbon plays an important role in the high visible-light activity of this carbon modified TiO_2. In addition, S450 has failed to remove even 10% MO. It can be explained by the result from the DRS tests, from which a 3.16 eV band gap is obtained and there is almost no absorption tail in the visible range.

It is necessary to consider the stability of carbon modified TiO_2 in the practical water purification application. The stability of the sample S350 was analyzed and the results shown in Fig. 10 display that the photocatalyst keeps activity after three cycling usages. All decrease efficiencies of MO are above 90%. The result suggests that the carbon modified TiO_2 is stable during the photocatalytic reaction.

To confirm the photocatalytic activity of the carbon modified TiO_2 and obtain more implication on the reaction mechanism, photoreduction of Cr(VI) over S350 under visible-light irradiation has been carried out. Here for the consideration of simultaneous photocatalytic degradation of bio-recalcitrant organic pollutants and reduction of Cr(VI), phenol is employed as a hole trapping agent in some cases. Table 1 shows the results in different conditions and the observed reaction rate constant k_{obs} was calculated based on the best linear fit to the data. The direct photoreduction of Cr(VI) is negligible in the absence of the catalyst. Moreover it also suggests that the Cr(VI) cannot oxidize phenol directly, and the photons have not changed the reaction state between phenol and Cr(VI). The adsorption of the Cr(VI) over the photocatalyst is also scarce. However, about 45.7% Cr(VI) have been reduced within 90 min in the presence of photocatalyst S350 upon visible-light irradiation. And the amount of Cr(VI) decreased was significantly promoted by the presence of phenol, as much as 92.7% Cr(VI) is reduced, and the removal rate increases twice. The effect of organics on the photocatalytic reduction of Cr(VI) has been investigated in detail in the references [55,56]. There exists synergistic effect on photocatalytic degradation of Cr(VI) and organic pollutants. The results suggest that the carbon modified TiO_2 prepared in this study could also be used as an efficient photocatalyst in Cr(VI) reduction. According to above discussion, upon visible-light irradiation, electrons are excited from the surface carbonaceous species, transferring out to the conduction band of TiO_2 and scavenged by oxygen or Cr(VI) for photocatalytic reaction.

4. Conclusion

Visible-light responsive carbon modified TiO_2 was successfully synthesized by a facile hydrolysis–precipitation–calcination approach, employing tetrabutyl titanate and water as reactants. According to the characterization results, the carbon elements in the sample calcined at 350 °C simultaneously presented as interstitial-doped carbon in the crystal lattice and graphite-like carbon on the surface. The sources of carbon were from the unhydrolyzed terminal butoxy group and adsorbed butanol. The excellent visible-light driven photocatalytic performance of this carbon modified TiO_2 in the degradation of methyl orange mainly resulted from a sensitization effect of graphite-like carbon. By optimizing the ratio of reactant, calcination temperature and oxygen concentration, the carbon modified TiO_2 with desired performance can be expected.

Acknowledgements

This work is financially supported by the Nanotechnology Program of Shanghai Science & Technology Committee (No. 0752nm007). The authors are grateful to Haibo Han of the Instrumental Analysis Center of Shanghai Jiao Tong University for XRD measurements and Wenfeng Shangguan of School of Environmental Science and Engineering, Shanghai Jiao Tong University for DRS and BET analysis.

References

[1] M.R. Hoffmann, S.T. Martin, W. Choi, D.W. Bahnemann, Chem. Rev. 95 (1995) 69–96.
[2] K. Maeda, K. Teramura, D. Lu, T. Takata, N. Saito, Y. Inoue, K. Domen, Nature 440 (2006) 295.
[3] P.V. Kamat, J. Phys. Chem. C 111 (2007) 2834–2860.
[4] F.E. Osterloh, Chem. Mater. 20 (2008) 35–54.
[5] A.L. Linsebigler, G. Lu, J.T. Yates, Chem. Rev. 95 (1995) 735–758.
[6] X. Chen, S.S. Mao, Chem. Rev. 107 (2007) 2891–2959.
[7] T. Cordero, J.-M. Chovelon, C. Duchamp, C. Ferronato, J. Matos, Appl. Catal. B: Environ. 73 (2007) 227–235.
[8] M.I. Litter, Appl. Catal. B: Environ. 23 (1999) 89–114.
[9] R. Asahi, T. Morikawa, T. Ohwaki, K. Aoki, Y. Taga, Science 293 (2001) 269–271.
[10] X. Hong, Z. Wang, W. Cai, F. Lu, J. Zhang, Y. Yang, N. Ma, Y. Liu, Chem. Mater. 17 (2005) 1548–1552.
[11] W. Zhao, W. Ma, C. Chen, J. Zhao, Z. Shuai, J. Am. Chem. Soc. 126 (2004) 4782–4783.
[12] L. Zang, C. Lange, I. Abraham, S. Storck, W.F. Maier, H. Kisch, J. Phys. Chem. B 102 (1998) 10765–10771.
[13] W. Zhao, C. Chen, W. Ma, J. Zhao, D. Wang, H. Hidaka, N. Serpone, Chem. Eur. J. 9 (2003) 3292–3299.
[14] Y. Cho, W. Choi, C.-H. Lee, T. Hyeon, H.-I. Lee, Environ. Sci. Technol. 35 (2001) 966–970.
[15] G. Liu, T. Wu, J. Zhao, H. Hidaka, N. Serpone, Environ. Sci. Technol. 33 (1999) 2081–2087.
[16] D. Mitoraj, H. Kisch, Angew. Chem. Int. Ed. 47 (2008) 9975–9978.
[17] S. Livraghi, M.C. Paganini, E. Giamello, A. Selloni, C.D. Valentin, G. Pacchioni, J. Am. Chem. Soc. 128 (2006) 15666–15671.

[18] C.D. Valentin, G. Pacchioni, A. Selloni, Phys. Rev. B 70 (2004) 085116.
[19] N. Serpone, J. Phys. Chem. B 110 (2006) 24287–24293.
[20] S.U.M. Khan, M. Al-Shahry, J. William, B. Ingler, Science 297 (2002) 2243–2245.
[21] H. Irie, Y. Watanabe, K. Hashimoto, Chem. Lett. 32 (2003) 772–773.
[22] D.-e. Gu, Y. Lu, B.-c. Yang, Y.-d. Hu, Chem. Commun. (2008) 2453–2455.
[23] W. Ren, Z. Ai, F. Jia, L. Zhang, X. Fan, Z. Zou, Appl. Catal. B: Environ. 69 (2007) 138–144.
[24] Y. Huang, W. Ho, S. Lee, Lizhi Zhang, G. Li, J.C. Yu, Langmuir 24 (2008) 3510–3516.
[25] X. Wang, S. Meng, X. Zhang, H. Wang, W. Zhong, Q. Du, Chem. Phys. Lett. 444 (2007) 292–296.
[26] Q. Xiao, J. Zhang, C. Xiao, Z. Si, X. Tan, Solar Energy 82 (2008) 706–713.
[27] S. Sakthivel, H. Kisch, Angew. Chem. Int. Ed. 42 (2003) 4908–4911.
[28] H. Wang, J.P. Lewis, J. Phys.:Condens. Matter 18 (2006) 421–434.
[29] C.D. Valentin, G. Pacchioni, A. Selloni, Chem. Mater. 17 (2005) 6656–6665.
[30] M. Toyoda, T. Yano, B. Tryba, S. Mozia, T. Tsumura, M. Inagaki, Appl. Catal. B: Environ. 88 (2009) 160–164.
[31] C. Lettmann, K. Hildenbrand, H. Kisch, W. Macyk, W.F. Maier, Appl. Catal. B: Environ. 32 (2001) 215–227.
[32] L.-W. Zhang, H.-B. Fu, Y.-F. Zhu, Adv. Funct. Mater. 18 (2008) 2180–2189.
[33] J. Matos, J. Laine, J.-M. Herrmann, Appl. Catal. B: Environ. 18 (1998) 281–291.
[34] J. Matos, A. Garcia, T. Cordero, J.-M. Chovelon, C. Ferronato, Catal. Lett. 130 (2009) 568–574.
[35] Z. Wang, W. Cai, X. Hong, X. Zhao, F. Xu, C. Cai, Appl. Catal. B: Environ. 57 (2005) 223–231.
[36] S.R.L. Inc., The Sadtler Standard NMR Spectra, Creative Chemists Science, Philadelphia, 1970 & 1974.
[37] D. Chen, Z. Jiang, J. Geng, Q. Wang, D. Yang, Ind. Eng. Chem. Res. 46 (2007) 2741–2746.
[38] S. Orlanducci, V. Sessa, M.L. Terranova, G.A. Battiston, S. Battiston, R. Gerbasi, Carbon 44 (2006) 2839–2843.
[39] A.C. Ferrari, J. Robertson, Phys. Rev. B 61 (2000) 14095–14107.
[40] H. Estrade-Szwarckopf, B. Rousseau, J. Phys. Chem. Solids 53 (1992) 419–436.
[41] B. Neumann, P. Bogdanoff, H. Tributsch, S. Sakthivel, H. Kisch, J. Phys. Chem. B 109 (2005) 16579–16586.
[42] H. Kamisaka, T. Adachi, K. Yamashita, J. Chem. Phys. 123 (2005) 084704.
[43] Y. Xie, X. Zhao, Y. Chen, Q. Zhao, Q. Yuan, J. Solid State Chem. 180 (2007) 3576–3582.
[44] F.B. Li, X.Z. Li, M.F. Hou, K.W. Cheah, W.C.H. Choy, Appl. Catal. A: Gen. 285 (2005) 181–189.
[45] D. Leinen, A. Fernández, J.P. Espinós, A.R. González-Elipe, Surf. Interface Anal. 20 (1993) 941–948.
[46] R. Beranek, H. Kisch, Photochem. Photobiol. Sci. 7 (2008) 40–48.
[47] F. Zhang, S. Jin, Y. Mao, Z. Zheng, Y. Chen, X. Liu, Thin Solid Films 310 (1997) 29–33.
[48] T. Bezrodna, G. Puchkovska, V. Shimanovska, I. Chashechnikova, T. Khalyavka, J. Baran, Appl. Surf. Sci. 214 (2003) 222–231.
[49] W.-C. Hung, S.-H. Fu, J.-J. Tseng, H. Chu, T.-H. Ko, Chemosphere 66 (2007) 2142–2151.
[50] A. Suárez-Gómez, R. Sato-Berrú, R.A. Toscano, J.M. Saniger-Blesa, F. Calderón-Piñar, J. Alloys Compd. 450 (2008) 380–386.
[51] H. Liu, A. Imanishi, Y. Nakato, J. Phys. Chem. C 111 (2007) 8603–8610.
[52] A. Chemseddine, T. Moritz, Eur. J. Inorg. Chem. 1999 (1999) 235–245.
[53] Y. Murakami, T. Matsumoto, Y. Takasu, J. Phys. Chem. B 103 (1999) 1836–1840.
[54] B.L. Bischoff, M.A. Anderson, Chem. Mater. 7 (1995) 1772–1778.
[55] J.M. Meichtry, M. Brusa, G. Mailhot, M.A. Grela, M.I. Litter, Appl. Catal. B: Environ. 71 (2007) 101–107.
[56] L. Wang, N. Wang, L. Zhu, H. Yu, H. Tang, J. Hazard. Mater. 152 (2008) 93–99.